Proc. Natl. Acad. Sci. USA
Vol. 89, pp. 1705–1709, March 1992
Biochemistry

Peptide mimetics of the thrombin-bound structure of fibrinopeptide A

(β-turn/molecular modeling)

HIROSHI NAKANISHI*, R. ALAN CHRUSCIEL†, RICHARD SHEN†, STEPHEN BERTENSHAW†, MICHAEL E. JOHNSON*, TIMOTHY J. RYDEL‡, ALEXANDER TULINSKY‡, AND MICHAEL KAHN†§

*Department of Medicinal Chemistry and Pharmacognosy, University of Illinois, P.O. Box 6998, Chicago, IL 60680; †Department of Chemistry (m/c 111), University of Illinois, P.O. Box 4348, Chicago, IL 60680; and ‡Department of Chemistry, Michigan State University, East Lansing, MI 48824

Communicated by Gilbert Stork, November 4, 1991

ABSTRACT **Recent work has suggested that the thrombin-bound conformation of fibrinopeptide A exhibits a strand–turn–strand motif, with a β-turn centered at residues Glu-11 and Gly-12. Our molecular modeling analysis indicates that the published fibrinopeptide conformation cannot bind reasonably to thrombin but that reorientation of two residues by alignment with bovine pancreatic trypsin inhibitor provides a good fit within the deep thrombin cleft and satisfies all of the experimental nuclear Overhauser effect data. Based on this analysis, we have successfully designed and synthesized hybrid peptide mimetic substrates and inhibitors that mimic the proposed β-turn structure. The results indicate that the turn conformation is an important aspect of thrombin specificity and that our turn mimetic design successfully mimics the thrombin-bound conformation of fibrinopeptide.**

The trypsin-like serine protease thrombin plays a critical role in thrombosis and hemostasis (1). Thrombin displays remarkable specificity, effecting the removal of fibrinopeptides A and B of fibrinogen through the selective cleavage of two Arg-Gly bonds among 181 Arg/Lys-Xaa bonds in fibrinogen (2). Significant advances have been made in recent years toward understanding the origin of specificity of the cleavage of the Arg^{16}-Gly^{17} bond of the Aα chain of human fibrinogen (3). Through kinetic analysis of synthetic substrates, Scheraga and collaborators (4) have demonstrated the importance of residues Asp-7 and Phe-8. Although this is consistent with the strong conservation of these sites in many species (5), it was initially difficult to reconcile the separation of these residues—9 and 10 amino acids removed from the scissile amide bond—with their dramatic effect on thrombin catalysis.

Recently, an experimental rationalization for this unusual specificity has been provided through NMR investigations of the complex between fibrinopeptide 7–16 and bovine thrombin (6). A striking feature that emerged in this work is the cluster of nonpolar residues—Phe-8, Leu-9, and Val-15—that are apparently brought into close proximity by the presence of a reverse turn centered around Glu-11 and Gly-12, as shown schematically below, with the arrow noting the scissile bond.

$$\begin{array}{l} \qquad\qquad\qquad\downarrow \\ Gly^{12}\text{-}Gly\text{-}Gly\text{-}Val\text{-}Arg\text{-}Gly^{17}\sim \\ \quad | \\ Glu^{11}\text{-}Ala\text{-}Leu\text{-}Phe\text{-}Asp^{7}\sim \end{array}$$

To examine the role that this proposed reverse turn plays in appositely orienting fibrinopeptide A in the thrombin active site, we have designed, synthesized, and evaluated the chimeric substrate **1**, which incorporates our previously reported β-turn mimetic framework (7). The (*R*, *R*) and (*S*, *S*) isomers of **1** accurately mimic the thrombin-bound conformation of fibrinopeptide A, as judged by their kinetic competency. The kinetic parameters for **1** are K_m = 149 μM, k_{cat} = 9.9×10^{-8} (M/min)(NIH unit/ml)$^{-1}$, and K_m = 47 μM, k_{cat} = 1.0×10^{-8} (M/min)(NIH unit/ml)$^{-1}$. By comparison, the values for the undecapeptide (AcPhe-Leu-Ala-Glu-Gly-Gly-Val-Arg-Gly-Pro-$NHCH_3$) and the 52-residue cyanogen bromide cleavage peptide of the fibrinogen α chain are K_m = 1100 μM, k_{cat} = 6.9×10^{-8} (M/min)(NIH unit/ml)$^{-1}$, and K_m = 47 μM, k_{cat} = 48×10^{-8} (M/min)(NIH unit/ml)$^{-1}$, respectively (4). The mimetic substrates are better than the undecapeptide and are comparable to the 52-residue peptide, particularly if one notes the effect of P_2' residues on k_{cat} (8). Thus, this approach may be generally useful for examining secondary structure specificity in the cleavage of prohormones and zymogens, where an important role for reversed turns is implicated (9–11).

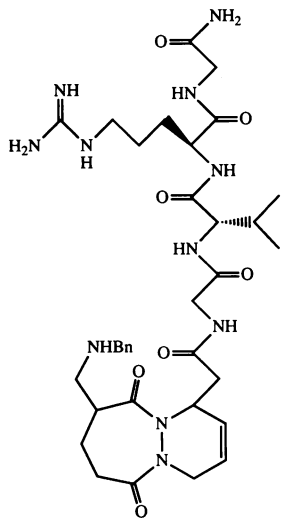

1

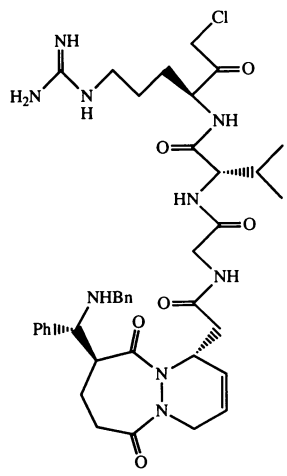

2

METHODS

Chimeric substrate **1**, described below, was synthesized by the procedure of Kahn and Bertenshaw (12) in a stereorandom fashion providing equal quantities of four diastereomers that were separated by reverse-phase HPLC. The synthesis of chloromethyl ketone inhibitor **2** is outlined in Fig. 1. The enantiospecific synthesis of **3** was accomplished as described (7), except that azetidinone **4** was prepared enantiospecifi-

The publication costs of this article were defrayed in part by page charge payment. This article must therefore be hereby marked "*advertisement*" in accordance with 18 U.S.C. §1734 solely to indicate this fact.

Abbreviation: BPTI, bovine pancreatic trypsin inhibitor.

§To whom reprint requests should be addressed.

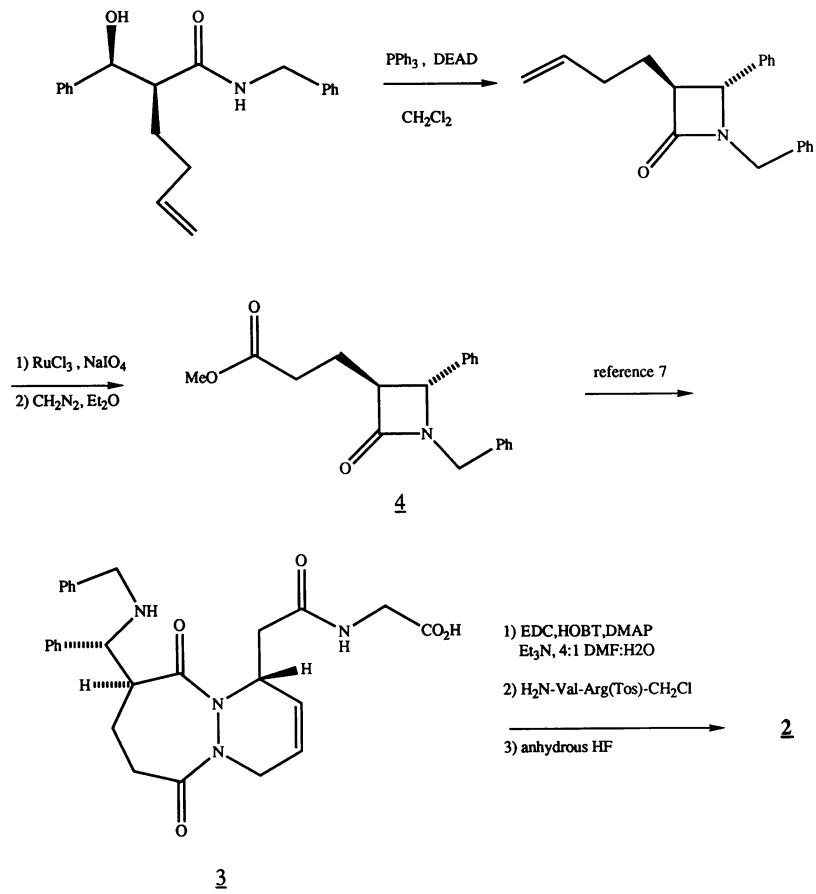

FIG. 1. Scheme for synthesis of 2. DEAD, diethylazodicarboxylate; EDC, 1-ethyl-3(3-dimethylaminopropyl)carbodiimide; HOBT, hydroxybenztriazole; DMAP, dimethylaminopyridine; DMF, dimethylformamide.

cally by the Evans protocol (13). Coupling to the valylarginyl chloromethyl ketone (14) and deprotection of the guanidinium group with anhydrous HF in the presence of anisole afforded 2. All new compounds were characterized by ^{1}H NMR (400 MHz), and MS (fast atom bombardment or plasma desorption mass spectrometry). Enantiomeric purity was assessed by ^{19}F NMR of the Mosher esters (15) and HPLC where appropriate. Kinetic parameters of the separated diastereomers were obtained by a standard HPLC assay (16). Cleavage products were correlated with independently synthesized authentic samples by HPLC analysis. Molecular models of the ring mimetics were built by the MacroModel molecular modeling program (17). Monte Carlo conformational searches for low-energy ring conformers utilized the Batchmin program, retaining only β carbons in the side chains. Each conformation was minimized by the MacroModel MM2 force field by the block diagonal Newton–Raphson method. The solvation effect was roughly taken into account by using a distance-dependent dielectric constant with a cutoff distance of 20 Å. Full models of the fibrinopeptide mimetics were then built from the lowest-energy ring conformations.

Table 1. Original ϕ, ψ angles calculated from the data in table III of Ni *et al.* (6) and modified backbone torsional angles of Val-15 and Arg-16 of fibrinopeptide 7–16

	Original		Modified	
Residue	ϕ	ψ	ϕ	ψ
Val-15	−92	28	−67	148
Arg-16	−101	−40	−105	37

RESULTS AND DISCUSSION

As the initial step in our investigations, we attempted to computationally dock the NMR-derived structure of fibrinopeptide 7–16 to the active site of thrombin by using the x-ray crystal structure obtained from the hirudin–thrombin complex (18) utilizing the atomic coordinates for the bound structure of the decapeptide (AcAsp-Phe-Leu-Ala-Glu-Gly-Gly-Gly-Val-Arg-NHCH$_3$) (6). Attempts to dock this sub-

Table 2. Comparison of interproton distances in the original fibrinopeptide reported by Ni *et al.* (6) and in the modified structure

Hydrogen pair	Bound, Å	Original	Modified
HN-Gly^{14}–Val^{15}-NH	>3.5	3.51	3.51
HB-Val^{15}–Arg^{16}-HN	>3.5	4.58	3.80
HN-HG Val^{15}	<2.5	2.08	2.15
HN-HB Arg^{16}	<2.5	2.36	2.40
HB-HE Arg^{16}	<2.5	2.57	2.57
HN-HB Val^{15}	<3.0	2.61	2.35
HN-HD Arg^{16}	<4.0	4.06	4.11
HA-Gly^{14}–Val^{15}-HN	<2.5	2.40	2.40
HA-Val^{15}–Arg^{16}-HN	<3.0	2.99	2.35
O-Gly^{13}–Arg^{16}-HN	2.2	1.95	2.20
HD-Phe^{8}–Gly^{14}-HA	<3.5	3.64	3.64
HE-Phe^{8}–Gly^{14}-HA	<3.0	2.55	2.55
HZ-Phe^{8}–Gly^{14}-HA	<3.5	3.40	3.40
HE-Phe^{8}–Val^{15}-HG	<3.0	2.10	2.19
HD-Phe^{8}–Val^{15}-HG	<3.5	3.61	3.49
HZ-Phe^{8}–Val^{15}-HG	<3.5	3.11	2.94

Only the distances affected by the torsional angle rotations given in Table 1 are listed.

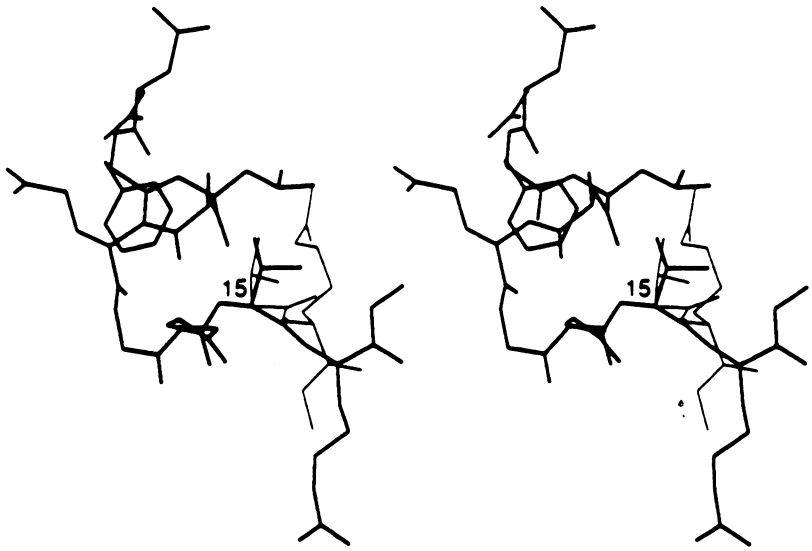

FIG. 2. Stereoview of the NMR-derived model for fibrinopeptide bound to thrombin. Original model is shown in thin lines; modified model is shown in heavy lines.

strate in the thrombin active site cleft, with Arg-16 in the S1 subsite, without massive collisions, were uniformly unsuccessful. Taking advantage of the striking similarity of the specificity pockets of thrombin and trypsin (19), and our belief that bovine pancreatic trypsin inhibitor (BPTI) is a mimic of a loop proteolysis substrate, we used the crystal structure of BPTI bound to trypsin (20) as a template to reorient fibrinopeptide 7–16 to allow for a bound complex. The α carbons of Gly-14, Val-15, and Arg-16 of fibrinopeptide were aligned with Pro-13, Cys-14, and Lys-15 of BPTI. The aligned fibrinopeptide structure was then superimposed with BPTI with a resulting rms deviation of 0.67 Å between the corresponding α carbon atoms. However, this alignment orients Arg-16 180° away from the S1 specificity pocket. To rectify this anomaly, the ϕ and ψ angles of Val-15 and Arg-16 were rotated. The original and modified torsional angles of the modified residues are given in Table 1; stereoviews of the original and modified structures are shown in Fig. 2. Importantly, this modification also satisfies all five intraresidue and the four sequential nuclear Overhauser effects for Val-15 and Arg-16 (Table 2). The modified fibrinopeptide fits well in the deep cleft of thrombin without further modification, as shown in Fig. 3.

Based on this analysis, we designed peptide chimeric substrate **1**. Two of the four diastereomers were substrates for human thrombin, although displaying moderately different kinetic profiles, as shown in Fig. 4, while the remaining two were resistant to enzymatic cleavage by thrombin. Trypsin effectively cleaved the Arg-Gly bond in all four diastereomers (data not shown). This highlights the role of the β-turn mimetic framework in appositely orienting the *N*-benzyl group with respect to the valine in the P_2 position of substrate **1**. This is critical for its cleavage by thrombin but is, not surprisingly, unimportant for trypsin. Molecular modeling readily rationalized these observations. The four diastereomers of the β-turn mimetic, respectively designated as (*S*, *S*), (*R*, *R*), (*S*, *R*), or (*R*, *S*), according to the chirality at carbon atoms C_1 and C_2 (Fig. 5), were constructed using MacroModel with the MM2/MMOD force field (17). The results of Monte Carlo conformational searches for the bicyclic ring are listed in Table 3. The lowest energy conformers for all the diastereomers have side-chain torsional angles incompatible with a β-turn. However, the (*R*, *R*) and (*S*, *S*) diastereomers have three conformers suitable for a β-turn that are only slightly above the lowest energy conformers. A rough estimate of the Boltzmann distribution at room temperature affords ≈50% of the structures with the

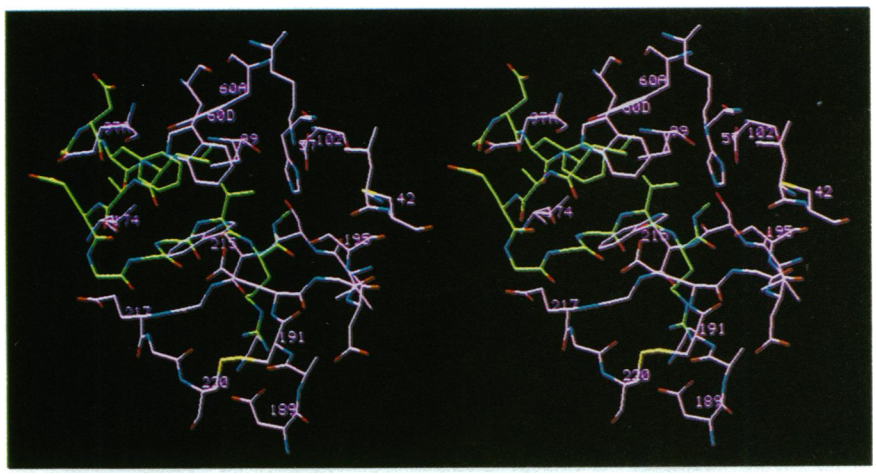

FIG. 3. Stereoview of the modified fibrinopeptide structure docked in the thrombin active site. Fibrinopeptide is shown in green; thrombin numbering is based on chymotrypsinogen (13).

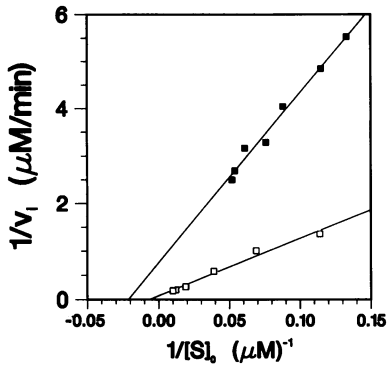

FIG. 4. Hydrolysis of the chimeric substrate 1 was carried out at 37°C in 0.1 M Tris·HCl buffer (pH 8.0) containing 0.1 M NaCl and 0.01 M $CaCl_2$ in a total vol of 50 μl with a thrombin concentration of 127 NIH units/ml (used as received from Sigma). Aliquots were removed and quenched by addition of 5% acetic acid and then immediately frozen and stored at −70°C until HPLC analysis was performed. The reaction aliquots were analyzed via reverse-phase HPLC (Synchropak RP-P-100; 0.46 × 25 cm). Elution was effected with a linear gradient of 10–40% acetonitrile containing 0.1% trifluoroacetic acid over a period of 30 min at a flow rate of 1.0 ml/min, with monitoring at 214 nm. Lineweaver–Burke plots are shown for the two purified substrates, yielding V_{max} = 13 μM/min, k_{cat} = 5.3 × 10^3 $M^{-1}\cdot s^{-1}$, and K_m = 149 μM for one diastereomer (□), and V_{max} = 1.3 μM/min, k_{cat} = 1.7 × 10^3 $M^{-1}\cdot s^{-1}$, and K_m = 47 μM for the other diastereomer (■). Stereochemistries for the two diastereomers are not yet assigned.

C_aC_1–C_2C_b dihedral angles in a range compatible with a β-turn conformation. The (*R*, *S*) and (*S*, *R*) diastereomers have no compatible structures within 5.8 kcal/mol (1 cal = 4.184 J) of the lowest conformer. From the nuclear Overhauser effect constraint data for fibrinopeptide 7–16 bound to thrombin, we obtain a value of −11° for the C_α^{10} $C(=O)^{10}$–$N^{13}C_\alpha^{13}$ dihedral angle (2). The rms deviations of the four carbon atom positions (C_a, C_1, C_2, and C_b) of the second lowest conformers for both the (*S*, *S*) and (*R*, *R*) diastereomers with respect to the corresponding atom positions [C_α^{10}, $C(=O)^{10}$, N^{13}, and C_α^{13}] of the fibrinopeptide bound structure are 0.16 and 0.25 Å, respectively, and the C_aC_1–C_2C_b dihedral angle is −13°. The ϕ, ψ torsional angles for the hybrid mimetics (*S*, *S*) and (*R*, *R*) were set to match those of the modified fibrinopeptide conformation, and the bicyclic rings of the mimetics were superimposed with the β-turn of the fibrinopeptide using the four carbon atom positions. The hybrid mimetic structures can then be readily docked to the thrombin active site, as shown in Fig. 6.

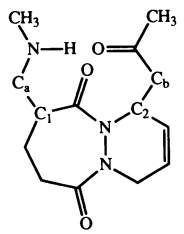

FIG. 5. Bicyclic ring system used as a turn mimetic for the design of fibrinopeptide mimetics. Four-atom $C_aC_1C_2C_b$ rms comparison and C_aC_1–C_2C_b dihedral angle comparison with the proposed modified fibrinopeptide conformation indicates that this mimetic exhibits a good fit to the proposed turn conformation.

This information has also been used to design and synthesize **2**, a potent, substrate-derived conformationally restricted hybrid mimetic inhibitor of thrombin that has K_{app}/I = 4.4 × 10^4 $M^{-1}\cdot min^{-1}$. (By comparison, we obtained a value of K_{app}/I = 1.6 × 10^7 $M^{-1}\cdot min^{-1}$ for the potent thrombin

Table 3. Results of Monte Carlo conformational searches for the four diastereomers of the bicyclic ring system (see Fig. 4) using the MM2/MMOD force field

Conformation	(*S*, *S*)		(*R*, *R*)		(*R*, *S*)		(*S*, *R*)	
	E	Angle	*E*	Angle	*E*	Angle	*E*	Angle
1	0.00	164	0.00	−164	0.00	95	0.00	−95
2	0.22	−13	0.22	13	0.58	114	0.58	−114
3	0.34	−2	0.34	2	1.10	131	1.10	−131
4	0.35	33	0.35	−33	1.34	99	1.34	−99
5	0.39	146	0.39	−146	1.81	97	1.81	−97
6	0.76	176	0.76	−176	2.04	110	2.04	−110
7	0.81	−44	0.81	44				
8	1.16	160	1.16	−160				
9	1.30	−28	1.30	28				
10	1.47	128	1.47	−128				
11	1.90	31	1.90	−31				

E, energy in kcal/mol; Angle, dihedral angle, C_aC_1–C_2C_b, in degrees. The distance between C_a and C_b, the mimetic C_α^i and C_α^{i+3} equivalents, varies from 5.1 to 5.6 Å for the (*S*, *S*) and (*R*, *R*) isomers and from 5.7 to 6.2 Å for the (*R*, *S*) and (*S*, *R*) isomers. Energies are calculated by using a distance-dependent dielectric but without explicit solvent. Thus, relative energetic ordering of the various conformers may change somewhat under more realistic solvent conditions. However, the existence of β-turn compatible conformations for the (*S*, *S*) and (*R*, *R*) isomers and the absence of β-turn compatible conformations for the (*R*, *S*) and (*S*, *R*) isomers should not be affected by these issues.

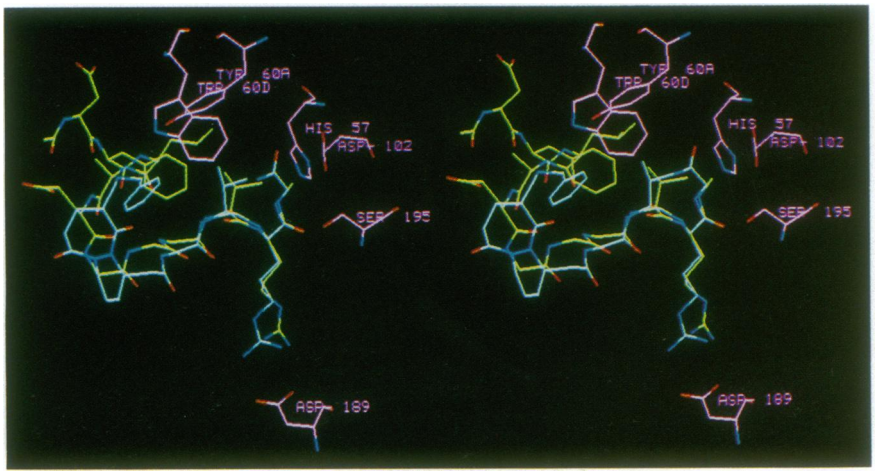

FIG. 6. Stereoview of proposed mimetic conformation of the (*R*, *R*) diastereomer (blue) shown overlapped with the modified NMR-derived bound conformation of fibrinopeptide A (green) within the thrombin active site.

inhibitor, (D)-phenylalanylprolylarginyl chloromethylketone.) Modeling for **2** indicates that the phenyl ring of the *N*-benzyl substituent can be easily positioned in the vicinity of the Val-15 side chain in a manner similar to the critical binding of the aromatic ring of Phe-8 of fibrinopeptide (data not shown). The chloromethyl ketone inhibitor, **2**, has crystallized with human thrombin in a tetragonal crystal system $a = b = 79.0$, $c = 160.9$ Å, space group $P4_122$ or $P4_12_12$, or enantiomorphs. The space group ambiguity resides in the fact that there is only one observed reflection along the *a* and *b* axes (10, 0, 0 and 0, 10, 0).

In conclusion, a coordinated attack utilizing crystallographic (18–20) and NMR data (4–6), computer-assisted molecular modeling, and organic synthesis has provided a highly plausible model for the bound structure of the extended peptide substrates of thrombin. Peptide mimetic substrates and inhibitors based on the proposed β-structure show significant specificity, providing corollary evidence for the proposed conformation. The structure of the thrombin mimetic complex should produce additional information on the importance of secondary structure in enhancing specificity of both macromolecules and their substrates.

We thank Prof. W. C. Still (Columbia University) for a copy of MacroModel. This work was supported in part by a Glaxo Cardiovascular Discovery grant to M.K. and M.J. and by National Institutes of Health Grant HL43220 to A.T. M.K. acknowledges the Searle Scholars Program/Chicago Community Trust for a Searle Scholars Award, the National Science Foundation for a Presidential Young Investigators Award, the Camille and Henry Dreyfus Foundation for a Teacher Scholar Award, American Cyanamid for a Faculty Development Award, and the American Heart Association for an Established Investigators Award.

1. Mann, K. G. (1987) *Trends Biochem. Sci.* **12**, 229–233.
2. Blombäck, H. (1967) in *Blood Clotting Enzymology*, ed. Seegers, W. H. (Academic, New York), pp. 143–215.
3. Scheraga, H. A. (1986) *Ann. N.Y. Acad. Sci.* **485**, 124–133.
4. Marsh, H. C., Jr., Meinwald, Y. C., Lee, S. & Scheraga, H. A. (1983) *Biochemistry* **22**, 4170–4174.
5. Henschen, A., Lottspeich, F., Kahl, M. & Southan, C. (1983) *Ann. N.Y. Acad. Sci.* **408**, 28–43.
6. Ni, F., Meinwald, Y. C., Vasquez, M. & Scheraga, H. A. (1989) *Biochemistry* **28**, 3094–3105.
7. Kahn, M., Wilke, S., Chen, B. & Fujita, K. (1988) *J. Am. Chem. Soc.* **110**, 1638–1639.
8. Fersht, A. R., Blow, D. M. & Fastrez, J. (1973) *Biochemistry* **12**, 2035–2041.
9. Rholam, M., Nicolas, P. & Cohen, P. (1986) *FEBS Lett.* **207**, 1–6.
10. Rholam, M., Cohen, P., Brakch, N., Paolillo, L., Scatturin, A. & DiBello, C. (1990) *Biochem. Biophys. Res. Commun.* **168**, 1066–1073.
11. Bek, E. & Berry, R. (1990) *Biochemistry* **29**, 178–183.
12. Kahn, M. & Bertenshaw, S. (1989) *Tetrahedron Lett.* **30**, 2317–2320.
13. Evans, D. A., Bartoli, J. & Shih, T. L. (1981) *J. Am. Chem. Soc.* **103**, 2127–2129.
14. Ketner, C. & Shaw, E. (1979) *Thrombosis Res.* **14**, 969–973.
15. Dale, J. A., Dull, D. L. & Mosher, H. S. (1969) *J. Org. Chem.* **34**, 2543–2549.
16. Beynon, R. J. & Bond, J. S., eds. (1989) *Proteolytic Enzymes: A Practical Approach* (IRL, Oxford).
17. Still, W. C. (1989) *Macromodel Interactive Modeling System (V3.1X)* (Department of Chemistry, Columbia University, New York).
18. Rydel, T. J., Ravichandran, K. G., Tulinsky, A., Bode, W., Huber, R., Roitsch, C. & Fenton, J. W., II (1990) *Science* **249**, 277–280.
19. Bode, W., Mayr, I., Baumann, U., Huber, R., Stone, S. R. & Hofsteenge, J. (1989) *EMBO J.* **8**, 3467–3475.
20. Huber, R. & Bode, W. (1978) *Acc. Chem. Res.*, 111–122.